CARMA Observations of Large Organic Molecules in Orion-KL

D.N. Friedel and L.E. Snyder
University of Illinois

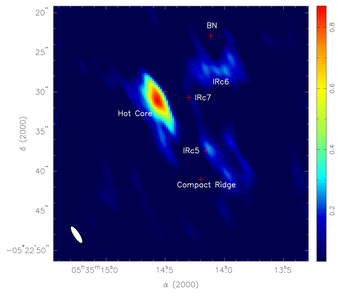

Fig. 1.—Continuum of Orion-KL at 231 GHz. Known infrared and radio sources are denoted with "+" and are labeled. The 1 σ rms noise level is 11.3 mJy bm^{-1}. The synthesized beam is in the lower left corner. Most of the continuum comes from the hot core (865 mJy bm^{-1} peak flux), however there is notable emission from IRc6 (232 mJy bm^{-1} peak flux), and there is also emission associated with IRc5 (254 mJy bm^{-1} peak flux) and IRc7 (101 mJy bm^{-1} peak flux). No emission was detected from either the compact ridge or BN, above our 1 σ rms noise level. There is, however, a notable hole in the continuum around the location of BN.

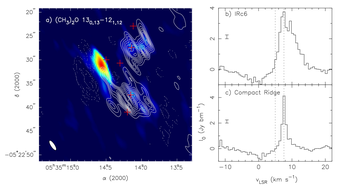

Fig. 2.— Map and spectra of C_2H_5CN. a) Map of the J=25$_{3,22}$ – 24$_{3,21}$, v_{LSR}=5.0 km s^{-1} emission overlaid on gray-scale continuum. Contours are ±3σ, ±5σ, ... (σ = 0.179 Jy bm^{-1}). The synthesized beam is in the lower left corner of the map and "+" marks denote the same sources as in the continuum map (see Figure 1). b) Spectra toward IRc7. Dashed lines mark v_{LSR}=5.0 and 7.6 km s^{-1} (typical rest velocities for this region). "I" bar denotes 1 σ rms noise level. c) Spectra toward the hot core.

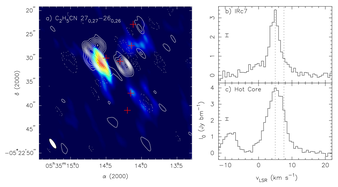

Fig. 3.— Map and spectra of $(CH_3)_2O$. a) Map of the J=13$_{0,13}$-12$_{1,12}$ v_{LSR}=7.6 km s^{-1} emission overlaid on gray-scale continuum. Contours are ±3σ, ±5σ, ... (σ = 0.252 Jy bm^{-1}). The synthesized beam is in the lower left corner of the map and "+" marks denote the same sources as in the continuum map (see Figure 1). b) Spectra toward IRc6. Dashed lines mark v_{LSR}=5.0 and 7.6 km s^{-1} (typical rest velocities for this region). "I" bar denotes 1 σ rms noise level. c) Spectra toward compact ridge.

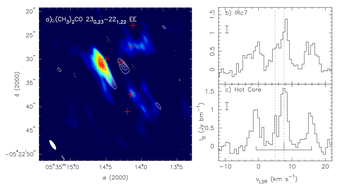

Fig. 4.— Map and spectra of $(CH_3)_2CO$. a) Map of the J=23$_{0,23}$ – 22$_{1,22}$ EE, v_{LSR}=5.0 km s^{-1} emission overlaid on gray-scale continuum. Contours are ±3σ, ±5σ, ... (σ = 0.196 Jy bm^{-1}). The synthesized beam is in the lower left corner of the map and "+" marks denote the same sources as in the continuum map (see Figure 1). b) Spectra toward IRc7. Dashed lines mark v_{LSR}=5.0 and 7.6 km s^{-1} (typical rest velocities for this region). "I" bar denotes 1 σ rms noise level c) Spectra toward hot core.

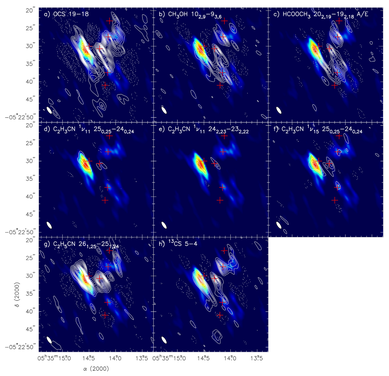

Fig. 5.— Maps from the transitions detected in the wideband windows(~500 MHz bandwidth, ~41.3 km s^{-1} resolution) overlaid on the continuum. Contours are ±3σ, ±5σ, ... (σ = 29 mJy bm^{-1}). The synthesized beam is in the lower left corner of the map and "+" marks denote the same sources as in the continuum map (see Figure 1). a) OCS J=19–18 emission. There are notable peaks and valleys all throughout the region indicating widespread features that are resolved out by the array, in addition to the smaller scale structures that are seen. For such a low temperature transition from a simple molecule this is not a surprising result. b) methanol [CH_3OH] J=10$_{2,9}$–9$_{3,6}$ emission. c) methyl formate [$HCOOCH_3$] J=20$_{2,19}$–19$_{2,18}$ A and E emission. d-f) show the $^1\nu_{11}$ J=25$_{0,25}$–24$_{0,24}$ and J=24$_{2,23}$–23$_{2,22}$ and $^1\nu_{15}$ J=25$_{0,25}$–24$_{0,24}$ transitions of vinyl cyanide [C_2H_3CN], respectively. g) C_2H_5CN J=26$_{1,25}$–25$_{1,24}$ emission. While this transition maps similarly to the other detected C_2H_5CN transitions there is one significant difference. The emission near IRc6 seen here is not detected in any other C_2H_5CN transitions. This may be due to contamination from weaker lines of O-bearing species (several acetaldehyde [CH_3CHO] transitions fell within the same channel). h) ^{13}CS J=5–4 emission.

Ethyl Cyanide
C_2H_5CN

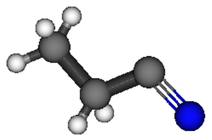

The observations were taken in 2007 March with the Combined Array for Research in Millimeter-Wave Astronomy (CARMA) at λ=1mm.

The typical synthesized beam was ~ 2.5″×0.85″

The correlator was configured to have two 500 MHz wide windows for continuum and four 32 MHz windows for spectral lines (half in each sideband). The spectral line windows had 63 channels with a spacing of 488 kHz (~0.64 km s^{-1}).

C_2H_5CN is a typical large N-bearing species and has been associated with the hot core for many years (e.g. Blake et al. 1987). Blake et al. (1996) and Beuther et al. (2005) showed an extension in C_2H_5CN emission toward IRc7.

The map of C_2H_5CN J=25$_{3,22}$ – 24$_{3,21}$ emission, shown in Figure 2a, clearly resolves this second component for the first time. It also shows an extended ridge of emission running northeast-southwest along the hot core and in the direction of known outflows.

Additionally, there is a peak of emission to the north of the hot core, a region which has no detected continuum emission. The emission from IRc7 may be coming from two (or more) partially resolved sources.

Figures 2b and c show the C_2H_5CN spectra toward IRc7 and the hot core, respectively. The second line (v_{LSR}~-9.5 km s^{-1}) in the hot core spectra may be a U-line or it may be a velocity component of C_2H_5CN. This line does not have a large spatial distribution and is confined to the southwest corner of the hot core.

While there is no notable velocity gradient along the ridge of the hot core there are some velocity gradients across the hot core near its southwestern tip. Figure 6 shows a position velocity (p-v) diagram of C_2H_5CN. The inset is a map of C_2H_5CN emission at a v_{LSR} of 5 km s^{-1} (a zoom in of Figure 2a). The line denotes the p-v cut and the "+" denotes the center position of the cut (α(J2000) = 05^{h}35^{m}14^s.4, δ(J2000) = −5°22′31″.5). The abscissa of the p-v diagram is offset arc seconds from the center point and the ordinate is v_{LSR} in km s^{-1}. The positions of the hot core and IRc7 are noted in the diagram as is the position of the U-line. The contours are the same as in Figure 2.

The hot core contains not only C_2H_5CN gas at 5.0 km s^{-1} but some higher velocity gas, near a v_{LSR} of 7.5 km s^{-1} (the typical compact ridge velocity). The diagram also shows that the hot core and IRc7 are connected by a ridge of lower velocity gas. This ridge also connects with the U-line indicating that it might be C_2H_5CN at a lower velocity. The U-line may also be the $^1\nu_6$ J=25−24 1e transition of HC_3N at 227.7916 GHz (Müller et al. 2005), a rather high energy line (Eu=859 K), which could explain its compactness.

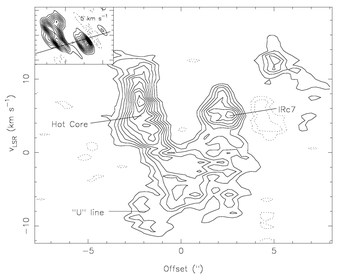

Fig. 6.— Position-velocity diagram of C_2H_5CN. The inset is a zoom in on the hot core/IRc7 emission, at a v_{LSR} of 5 km s^{-1}, shown in Figure 6. The line denotes the p-v cut and the "+" denotes its center (α(J2000) = 05^{h}35^{m}14^s.4, δ(J2000) = −5°22′31″.5). The abscissa of the diagram is offset arcseconds from the p-v center and the ordinate is v_{LSR} in km s^{-1}. Labels indicate the position of the hot core and IRc7 along with the potential U-line. The contours are the same as those in Figure 2.

Dimethyl Ether
$(CH_3)_2O$

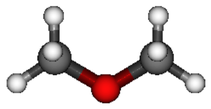

$(CH_3)_2O$ is a typical large O-bearing species and has been associated with the compact ridge (e.g. Liu et al. 2002).

Figure 3a shows the map of the J=13$_{0,13}$-12$_{1,12}$ transitions of $(CH_3)_2O$ at a v_{LSR} of 7.6 km s^{-1}. There is significant emission from IRc6 with a notable hole near Orion-BN, and in regions near IRc5. However, there is no notable emission from the compact ridge itself.

Also there is some emission from the hot core-SW. This emission is similar to that seen by Beuther et al. (2005) at 865 μm, however they do not see the "C" shape around BN, but rather see more point like emission from IRc6. This may be explained by the factor of ~2 difference in E_u between the observed transitions.

Figures 3b and c show the $(CH_3)_2O$ spectra from IRc6 and IRc5, respectively.

Acetone
$(CH_3)_2CO$

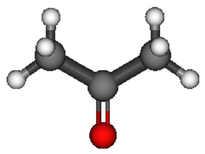

$(CH_3)_2CO$, while a large O-bearing species, does not map like any of the other molecules we observed.

Figure4ashowsamapofthe$(CH_3)_2CO$$J$=23$_{0,23}$−22$_{1,22}$ EE emission. Two distinct emission features are seen. One at hot core-SW, the other near IRc7. Figures 4b and c show the spectra toward IRc7 and the hot core, respectively.

All three spectral features (AE/EA, EE, & AA) are seen at both positions. Both spectra are best fit by two velocity components, ~5 km s^{-1} and ~8 km s^{-1}, typical v_{LSR} values for the hot core and compact ridge. This is the largest known molecule that shows both velocity components, which are co-spatial at our resolution.

Unlike C_2H_5CN there are no velocity gradients in any of the $(CH_3)_2CO$ emission.

Conclusions

Some have argued that the differentiation may be due to the dipole/critical density differences between C_2H_5CN and $(CH_3)_2O$. This is not likely to be the case in this region (see Friedel & Snyder 2008).

Others have argued that the differentiation could be due to differences in the age of the regions, the O-bearing species are liberated off grain surfaces by shocks or form in gas phase reactions in shocked regions, while the N-bearing species take longer to form in gas-grain reactions (e.g. Blake et al. 1987). This argument fits well with what is suspected about the region: outflows from the older (N-bearing) hot core are impacting the ambient gas and dust forming shocked regions where larger O-bearing species are most populous.

However, our observations of $(CH_3)_2CO$ show that this O-N differentiation is not as simple as it may seem. Figure 7 shows C_2H_5CN in red contours, $(CH_3)_2O$ in green contours, and $(CH_3)_2CO$ in black contours, overlaid. It shows that the $(CH_3)_2CO$ emission comes only from regions where both $(CH_3)_2O$ and C_2H_5CN overlap.

If we assume that the age difference argument is correct then it would seem that it takes significant processing (either on grain surfaces or in the gas phase) to form $(CH_3)_2CO$, but that it is also short lived as it seems to not be present in older regions where N-bearing molecules dominate. Recent models by Garrod, Widicus Weaver, & Herbst, in preparation, indicate that this may be true: $(CH_3)_2CO$ forms where the warm-up time scale is longer, indicating grain surface formation from reactions with secondary products.

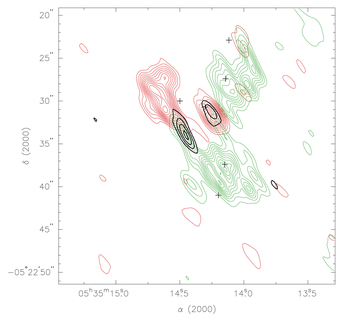

Fig. 7.— Overlaid maps of C_2H_5CN in red contours, $(CH_3)_2O$ in green contours, and $(CH_3)_2CO$ in black contours. Note that negative contours have been removed to reduce confusion. The $(CH_3)_2CO$ emission only appears where both C_2H_5CN and $(CH_3)_2O$ emission overlap.

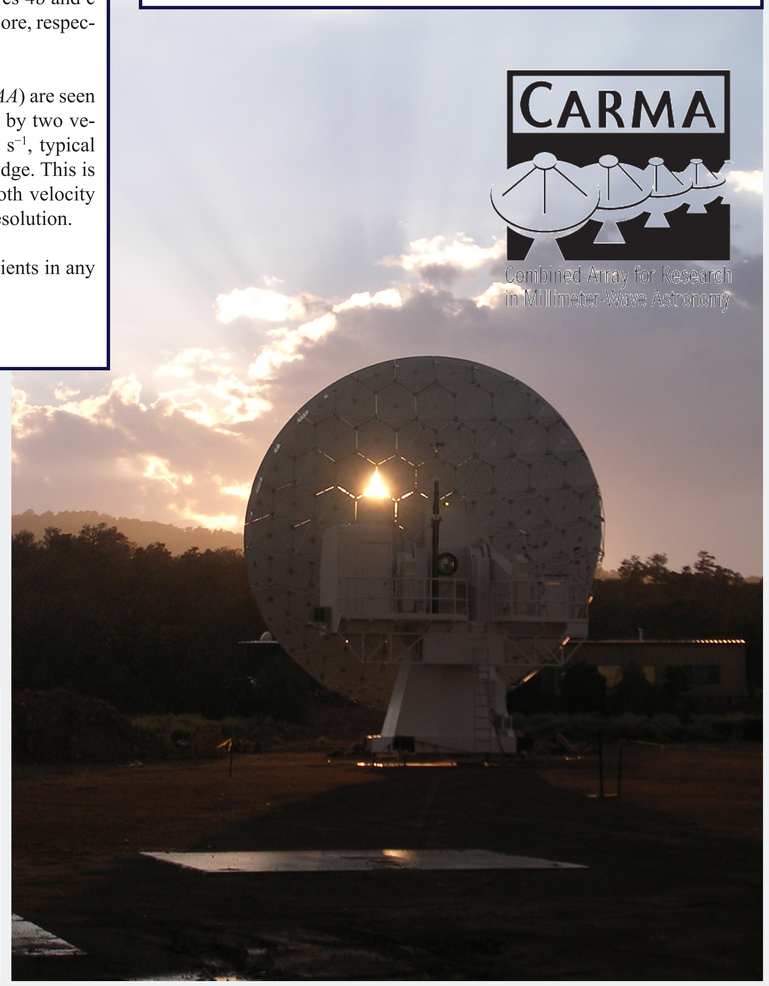

References

Beuther, H., et al. 2005, ApJ, 632, 355
Blake, G. A., Sutton, E. C., Masson, C. R., & Phillips, T. G. 1987, ApJ, 315, 621
Blake, G. A., Mundy, L. G., Carlstrom, J. E., Padin, S., Scott, S. L., Scoville, N. Z., & Woody, D. P. 1996, ApJ, 472, L49
Friedel, D. N. & Snyder, L. E. 2008, ApJ, in press
Liu, S., Girart, J. M., Remijan, A., & Snyder, L. E. 2002, ApJ, 576, 255
Müller, H. S. P., Schlöder, F., Stutzki, F., & Winnewisser, G. 2005, J. Mol. Struct. 742, 215

This work was partially funded by NSF grant AST-0540459 and the University of Illinois.